DAMAGE TOLERANCE AND ENGINEERING PROPERTIES OF ALUMINIUM-LITHIUM ALLOYS

W.G.J. 't Hart, L. Schra and R.J.H Wanhill
National Aerospace Laboratory NLR
8300 AD Emmeloord, The Netherlands

Abstract

The damage tolerance (fatigue and fracture) and engineering properties of commercial aluminium-lithium alloys are evaluated and compared with those of the conventional aerospace alloys. The new aluminium-lithium alloys have considerable potential for replacing conventional materials. However, their engineering property behaviour can be significantly different. A much more detailed understanding of the mechanical and environmental behaviour of aluminium-lithium alloys is required than might be expected. This paper presents results from several years' investigation at the NLR, and problem areas are defined and discussed.

1. Introduction

The tremendous effort to develop aluminium-lithium alloys for aerospace applications has now reached the stage that different types of Al-Li alloys are becoming available from major alloy producers. The aluminium producers Alcoa, Alcan and Cegedur Pechiney have introduced a number of Al-Li alloys as potential replacements for the damage tolerant alloy 2024-T3, the medium strength alloy 2014-T6 and the high strength alloy 7075-T6 (1-3). Before acceptance of a new alloy for aerospace structures an extensive qualification programme has to be done by potential users.

The National Aerospace Laboratory (NLR) has concentrated mainly on the damage tolerant properties of Al-Li alloys. The present paper presents the results of an experimental investigation of damage tolerant Al-Li sheet materials from Alcan and Pechiney and a medium strength plate alloy from Alcan. Results are compared with the similarly determined properties of 2024-T3 sheet and 2024-T351 plate.

2. Materials and experimental programme

For investigation of thick plate properties Alcan supplied 25 mm thick plate of the medium strength alloy 8090-T651 and Alcoa supplied 30 mm thick 2024-T351 plate. Damage tolerant 1.6 mm thick Al-Li sheet materials were supplied by Alcan (8090C-T81) and Cegedur Pechiney (2091-T8X). Both sheet materials were unclad and in a recrystallized condition. For comparison 2024-T3 sheet from Alcoa was used. Chemical compositions of the alloys are given in table 1. Note that the Li content of 2091 is lower than that for 8090 but the copper content is higher. This means that Cu is the main alloying element, making the Pechiney material a 2000 series alloy. In both Al-Li alloys Zr is added as a grain refiner.

An overview of the test programme is given in table 2. Tensile properties were determined for different loading directions using specimens dimensioned according to ASTM Standard B 557-81. Short transverse tensile properties of plate were established from tests on specimens 3.2 mm in diameter. Compact tension fracture toughness specimens according to ASTM Standard E399-81 were used for K_{Ic} tests on plate materials, and 500 mm wide centre cracked panels were used for residual strength tests on sheet materials. Constant amplitude and flight simulation fatigue crack growth tests were performed on 2 and 10 mm thick specimens taken from plate and 1.6 mm thick sheet specimens. S-N curves were produced for 4 mm thick notched (K_t = 3.1) specimens from plate and 1.6 mm thick notched (K_t = 2.5) sheet specimens. Stress corrosion and general corrosion properties were determined under outdoor exposure conditions and in accelerated corrosion tests. For plate materials Double Cantilever Beam (DCB) type specimens were used to investigate the resistance to stress corrosion crack growth, and tuning fork type specimens were used to determine the stress corrosion crack initiation lives. The stress corrosion behaviour of sheet materials was examined by exposing bent strips of 20 x 200 mm to the corrosive environment. More details on all the test specimens are given in references (4,5).

Materials	Cu	Mg	Li	Mn	Zn	Cr	Ti	Zr	Fe	Si
8090-T651 plate	1.24	0.60	2.42	0.00	0.00	0.00	0.05	0.12	0.12	0.05
2091-T8X sheet	2.10	1.60	1.80	-	-	-	0.02	0.07	0.04	0.03
8090C-T81 sheet	1.20	0.71	2.38	0.001	0.02	0.001	0.02	0.11	0.03	0.03
2024-T3 sheet }	3.8-	1.2-	-	0.3-	0.25	0.1	-	-	0.50	0.50
2024-T351 plate }	4.9	1.8		0.9	max	max			max	max

TABLE 1 CHEMICAL COMPOSITIONS OF THE INVESTIGATED PLATE AND SHEET MATERIALS:
(1) producers data for Al-Li alloys;
(2) Aluminium Association limits for 2024-T3 and T351

Mechanical properties	• Tension tests in L, T and S directions
Fracture toughness	• Fracture toughness tests on Compact Tension specimens for LT, TL, ST and SL orientations • Fracture toughness tests on Centre Cracked wide panels
Fatigue properties	• Fatigue crack growth tests on Centre Cracked Tension specimens under constant amplitude and flight simulation loading for the LT orientation • Constant amplitude notched fatigue tests (K_t = = 3,1 or 2.5) to obtain S-N curves between 10^4 and 3 x 10^7 cycles
Stress corrosion properties	• Constant strain stress corrosion crack initiation tests on tuning fork type specimens, SL orientation (plate), and on bent sheet strips, loaded in T-direction. Environments: - outdoor exposure, rural atmosphere - alternate immersion in synthetic seawater • Stress corrosion crack growth tests on Double Cantilever Beam specimens, SL orientation. Environments: - outdoor exposure, rural atmosphere - alternate immersion in synthetic seawater
Corrosion	• Susceptibility to corrosive attack under - EXCO-testing - intermittent salt spray testing, MASTMAASIS - outdoor exposure, rural atmosphere

TABLE 2 SURVEY OF EXPERIMENTAL PROGRAMME

3. Mechanical properties and fracture toughness

Average mechanical property data for plate and sheet are given in figure 1. The mean UTS of the medium strength plate alloy 8090 and 2024 plate was similar (~ 490 MPa) for the L and T directions. The 0.2 % TYS for 8090-T651 was significantly higher than that of 2024-T351 for all test directions. However, the elongation to fracture of 8090-T651 was less than half that of 2024-T351.

Comparing the strength properties of the sheet materials shows that 8090C-T81 and 2091-T8X had comparable UTS values (~ 440 MPa) which were substantially lower than that of 2024-T3 (490 MPa). The 0.2 % TYS of Al-Li sheet alloys was slightly lower than that of 2024-T3. The elongation to fracture of 2091-T8X was considerably higher than that for 8090C-T81 (14 % vs. 7 %) but still lower than that for 2024-T3 (17 %).

Fracture toughness data for plate and sheet are plotted in figure 2. To enable fracture toughness tests in the short transverse direction of the plate small compact tension specimens with a thickness of 10 mm were tested. Tests on 24 mm thick specimens showed similar K_{Ic} values for 8090 and 2024 plate*. The most conspicuous feature is the decrease in fracture toughness when 8090 is loaded in the short transverse direction. For this orientation the K_{Ic} was less than 40 % of the K_{Ic} for the LT or TL orientation. Although no tests in the short transverse direction were performed on 2024-T351 plate, literature data (Refs. 6 and 7)

* Minor violations for valid K_{Ic} values necessitate reporting K_Q values

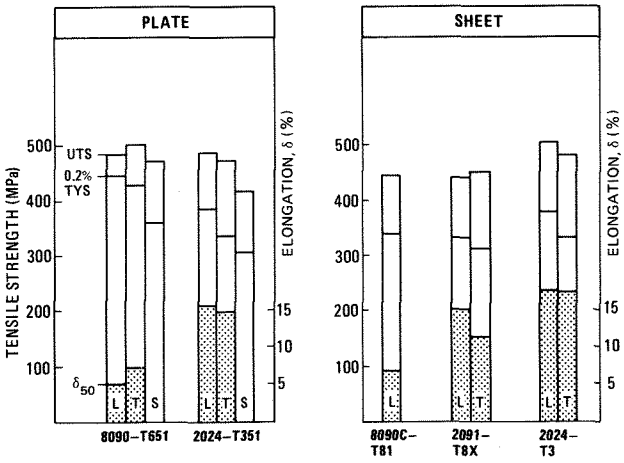

Fig. 1 Survey of mechanical properties

give values of 60 % of the fracture toughness for the LT or TL orientation.

Residual strength tests were executed according to ASTM Spec. E561-81. During the displacement controlled tests an anti-buckling guide was used. Initial crack lengths of $2a_o$ = 100 and 156 mm were applied. The fracture toughness K_c was calculated from

$$K_c = \sigma_c \sqrt{\pi\, a_c \sec \frac{\pi a_c}{w}}$$

where

K_c = plane stress fracture toughness

σ_c = gross stress at maximum load

a_c = physical half crack length at σ_c

$\sqrt{\sec \frac{\pi a_c}{w}}$ = finite width correction according to Feddersen

From figure 2 it can be seen that the K_c values for 2091-T8X and 8090C-T81 were 5 and 10 % lower than those for 2024-T3. In figure 3 the K_c values are plotted as a function of the 0.2 % TYS and some

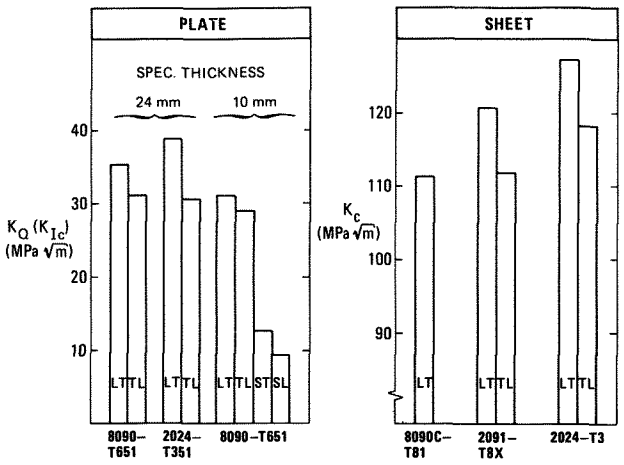

Fig. 2 Comparison of fracture toughness properties

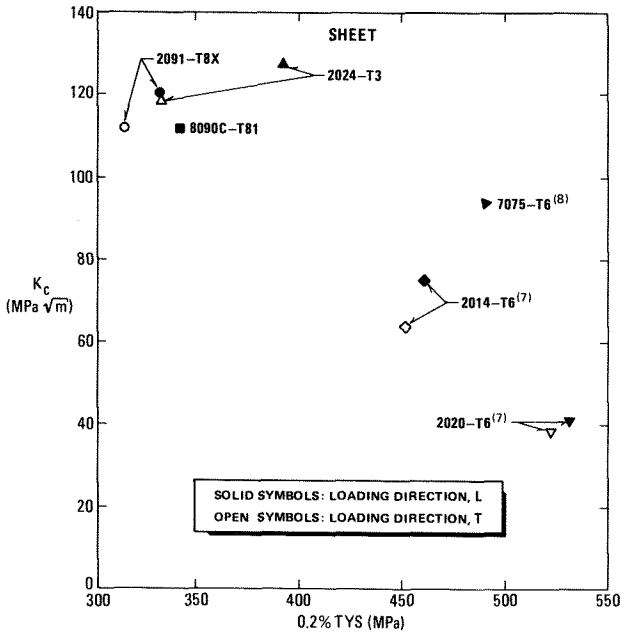

Fig. 3 Fracture toughness performance of sheet materials

literature data are indicated for comparison. The damage tolerant materials combine high toughness with low 0.2 % TYS values. It is seen that the precociously developed Al-Li alloy 2020-T6, which was withdrawn from production in 1974, does not belong to the group of damage tolerant materials.

4. Fatigue

4.1 Notched fatigue strength

Constant amplitude fatigue tests were carried out at a stress ratio of R = 0.1 on specimens with a theoretical stress concentration factor K_t = 3.1 (plate) and K_t = 2.5 (sheet). Notched fatigue tests give information on the fatigue behaviour of structural materials with e.g. fastener holes. Figure 4 shows the results. The maximum fatigue stress levels were selected such that S-N curves between 10^4 and 3×10^7 cycles could be constructed. The fatigue strength at 10^7 cycles was

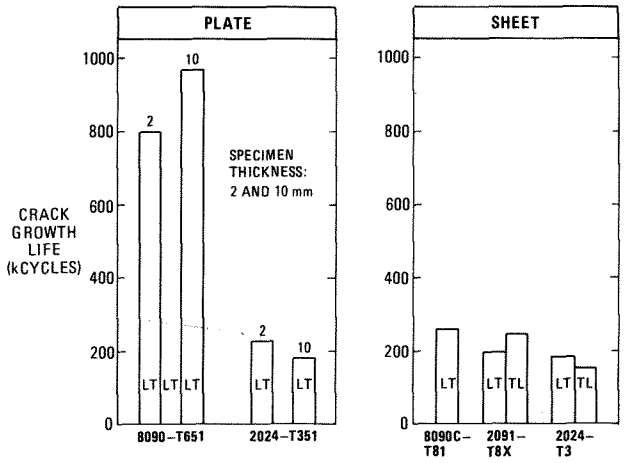

Fig. 5 Constant amplitude crack growth results at S_{max} = 70 MPa, R = 0.1

considerably higher (by about 20 %) for 8090-T651 and 2091-T8X than for 2024-T3 and T351. The fracture surfaces of the 8090-T651 specimens were somewhat unusual. They showed
- a lamellar appearance
- fatigue crack initiation at several locations
- rubbing characteristics (black deposits) for low S_{max} values.

4.2 Fatigue crack growth

Two types of fatigue loading were used: constant amplitude with R = 0.1 and S_{max} = 70 MPa and the gust spectrum MINITWIST with a mean stress in flight of S_{mf} = 70 MPa. Centre cracked tension (CCT) specimens were used with an initial crack length of $2a_o$ = 8 mm. During the flight simulation tests buckling of the 2 mm and 1.6 mm thick specimens during compression loading was prevented by felt-lined aluminium alloy anti-buckling guides with cutouts for visual observation of the cracks.

Constant amplitude results

Crack growth lives for plate and sheet materials are plotted as a bar chart in figure 5. For plate the mean crack growth lives of core and surface material are indicated. The large difference in

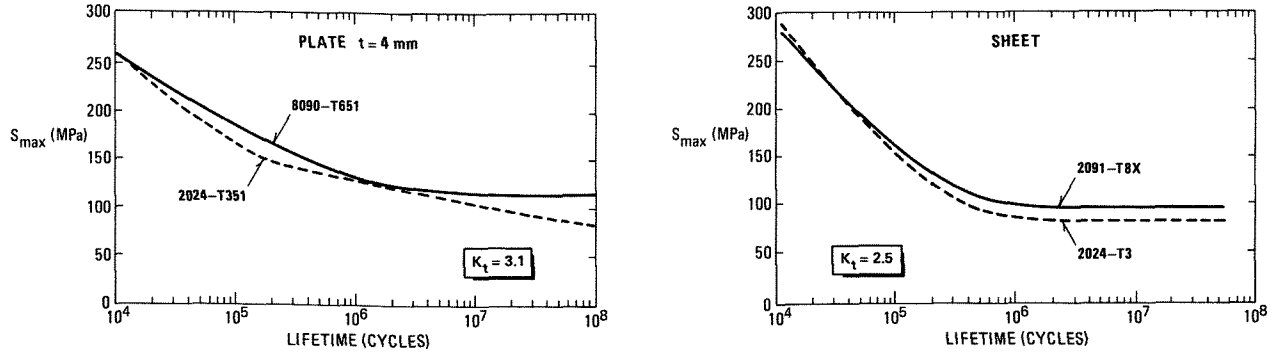

Fig. 4 Results of constant amplitude notched fatigue tests at R = 0.1 (mean S-N curves for core and surface material from plate)

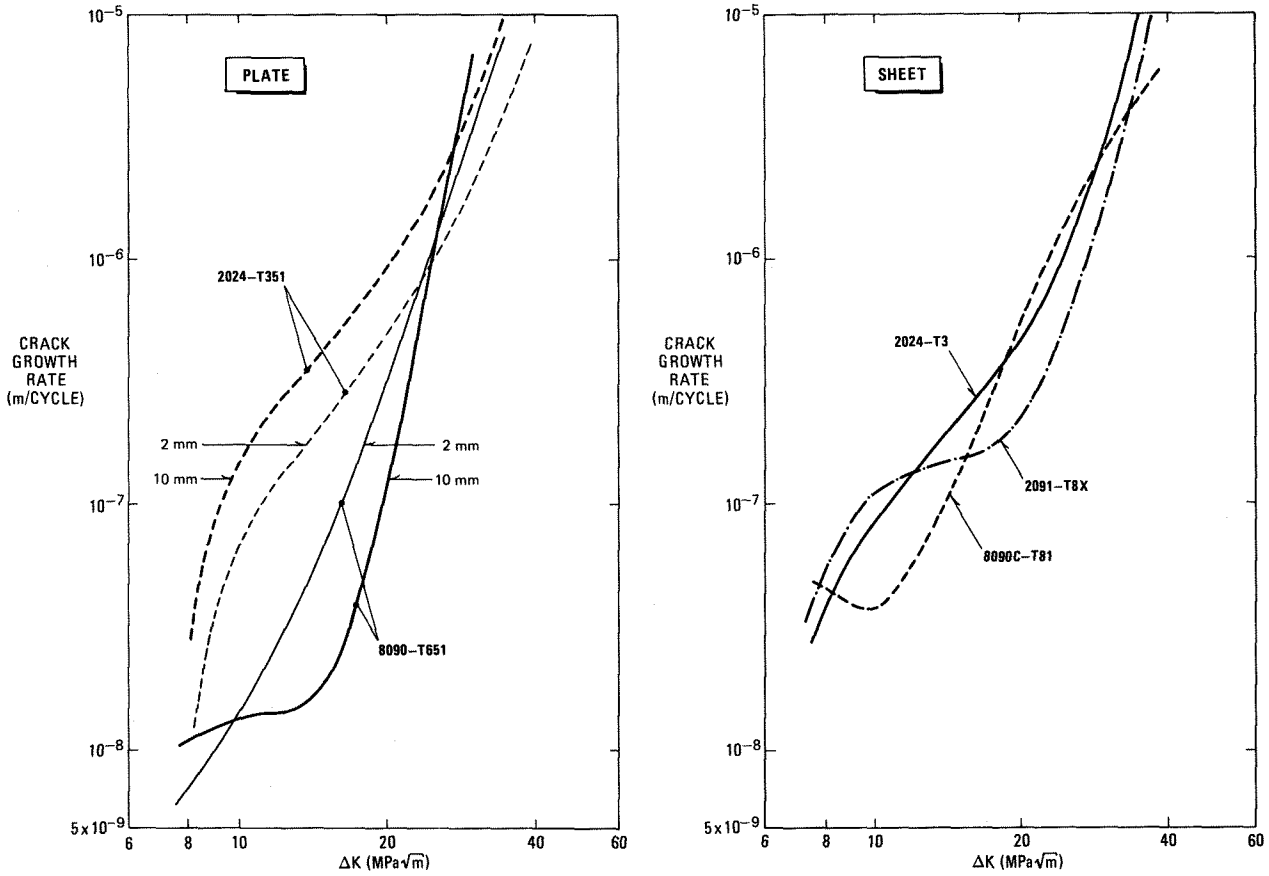

Fig. 6 Constant amplitude fatigue crack growth rates (R = 0.1): LT orientation

fatigue life for 2 and 10 mm thick specimens of 8090-T651 and 2024-T351 is striking. The difference in crack propagation life was about a factor 5. Also the crack propagation life of medium strength 8090-T651 plate was much higher than that of the damage tolerant Al-Li alloy sheet materials. The crack propagation lives of 8090C-T81 and 2091-T8X sheet were about 10 to 20 % longer than that of 2024-T3 sheet. Crack propagation rates as a function of the stress intensity range ΔK, figure 6, show that for the plate alloys the crack growth rate is far less in 8090-T651 than in 2024-T351, especially for the ΔK range of 8 - 20 MPa√m. The fracture surfaces of the 8090-T651 specimens showed

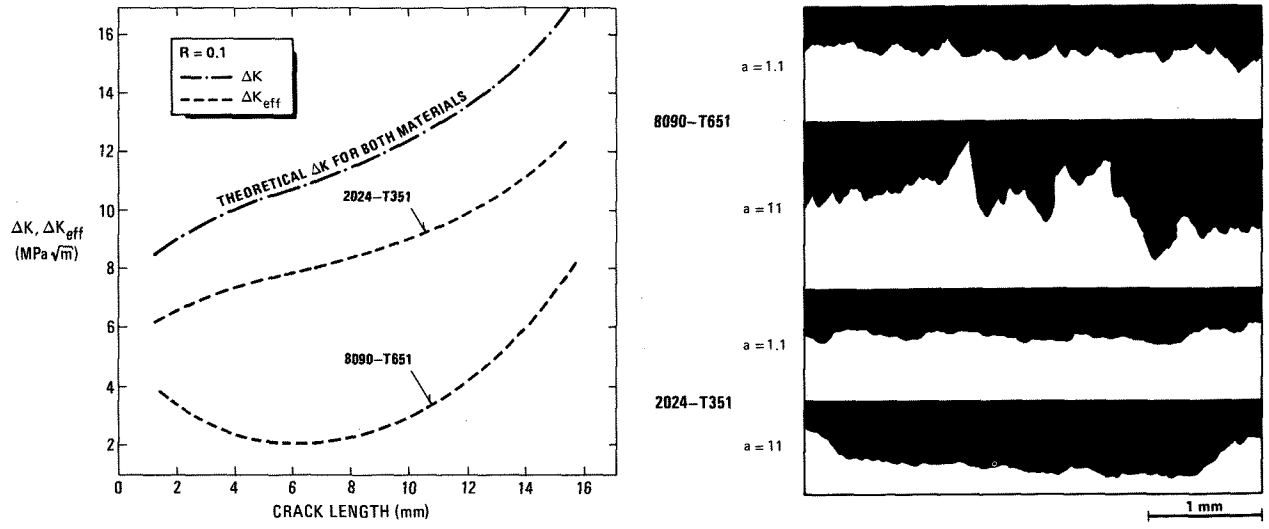

Fig. 7 ΔK_{eff} derived from crack opening measurements and the fracture surface roughness profiles for different crack lengths

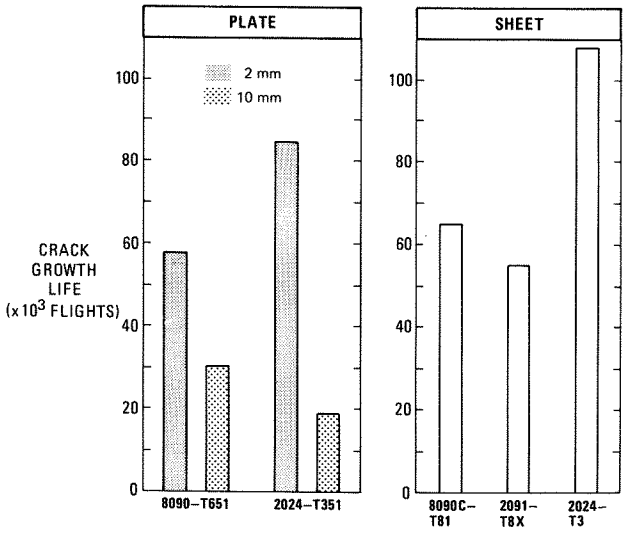

Fig. 8 Comparison of fatigue crack growth lives for gust spectrum loading (MINITWIST; truncation level III; S_{mf} = 70 MPa; LT orientation)

a lamellar appearance and black deposits indicating rubbing during fatigue testing. This indicates a higher crack opening stress and reduced effective stress intensity range. To verify this, additional crack growth tests were performed on 4 mm thick Single Side Cracked Hole (SCCH) specimens (4) of the plate materials. During fatigue testing load - Crack Opening Displacement (COD) measurements were made at regular crack length intervals to establish the crack opening stress and the stress intensity for which the crack is fully open (= K_{op}). Thus a plot could be made of the theoretical ΔK (= K_{max}-K_{min}) and ΔK_{eff} (= K_{max}-K_{op}) as functions of the crack length. To visualize the surface roughness cross-sections were made after fatigue testing for different crack lengths. Figure 7 shows that ΔK_{eff} is far smaller for 8090-T651 than for 2024-T351 and that a smaller ΔK_{eff} is accompanied by rougher fracture surfaces. Thus the excellent C.A. fatigue crack growth behaviour of 8090-T651 can be explained by a surface roughness induced phenomenon.

The shape of the crack growth rate curves for 8090C-T81 and 2091-T8X can also be explained on account of surface roughness effects. The initially decreasing crack growth rate of 8090C-T81 was accompanied by early development of surface roughness. Alloy 2091-T8X started with a smooth fracture surface and developed surface roughness in a later stage. This resulted in the sigmoidal trend shown in figure 6.

Flight simulation results

The gust spectrum MINITWIST is a shortened version of the standardized gust spectrum TWIST (Transport WIng STandard) and consists of blocks of 4000 flights. Details of the spectrum can be found in references (9,10). For the present investigation peak loads in the spectrum were truncated to a level of 8 occurrences per block of 4000 flights (truncation level III). This is a reasonable truncation level for crack propagation testing (11).

Comparison of fatigue crack growth lives for gust spectrum loading, figure 8, shows that for 2 mm and 1.6 mm thick sheet specimens 2024 was superior to the Al-Li alloys. However, for 10 mm thick plate specimens the fatigue life of 2024-T351 was shorter than that of 8090-T651. Mean crack propagation rate curves, figure 9, show constant or decreasing crack propagation rates for the 2 mm and 1.6 mm thick specimens. Decreasing crack propagation rates are a consequence of transient crack growth behaviour that results from the crack growth retarding effect of peak loads in severe flights in the gust spectrum. The effect is more pronounced under plane stress (or mixed plane

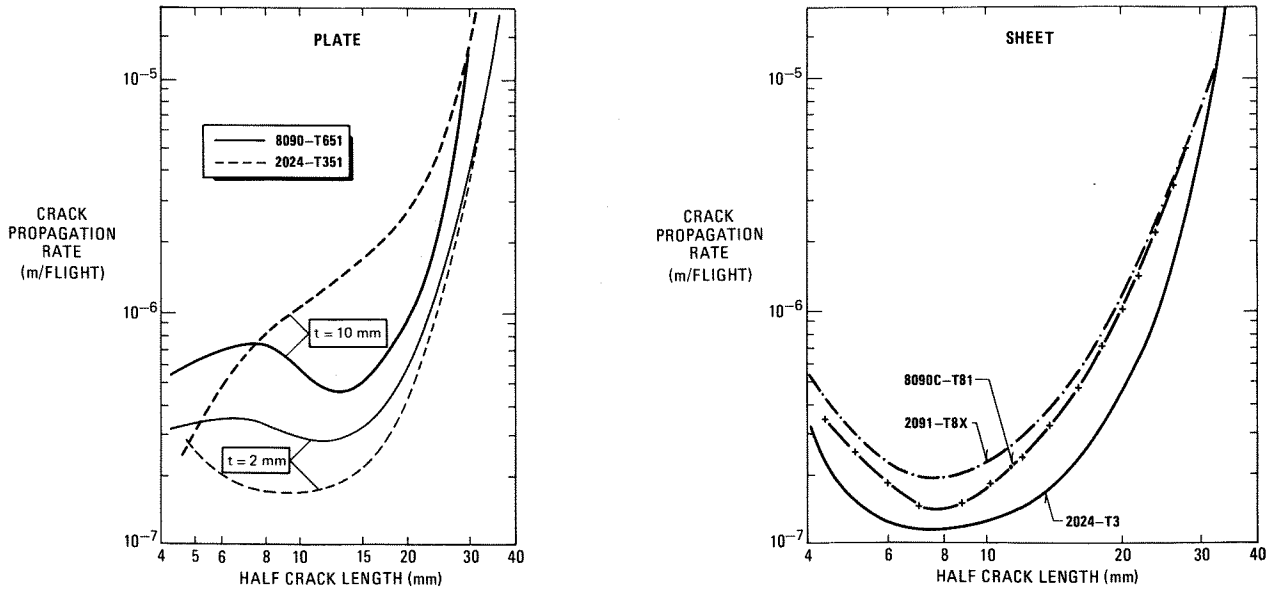

Fig. 9 Comparison of crack propagation rates under gust spectrum loading (MINITWIST ; truncation level III; S_{mf} = 70 MPa; LT orientation)

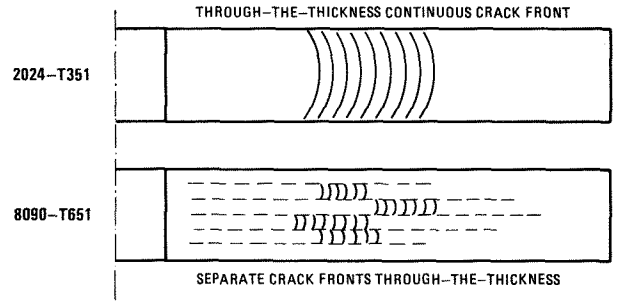

Fig. 10 Fracture surface appearances of 10 mm thick specimens after gust spectrum loading

strain - plane stress) conditions than under predominantly plane strain conditions (10 mm thick specimens). In the former situation larger peak load plastic zones develop, resulting in greater changes in crack closure. The crack growth retardation is most pronounced for the 2024-T3 sheet material and explains the superior crack growth life.

The more or less constant crack growth rate for the 10 mm thick 8090-T651 specimens is attributed to a different phenomenon, as was deduced from the fracture surfaces. On the fracture surfaces of 8090-T651 there were signs of separate crack fronts through-the-thickness, schematically shown in figure 10. This may be attributed to the poor short transverse properties enabling internal delamination during fatigue crack growth. The fatigue behaviour is then more representative for a laminated structural material than for a monolithic solid plate. In figure 9 it is seen that at the start of crack propagation the crack propagation rate increased up to a crack length of 7 mm. Up to this crack length the separate crack fronts had not fully developed.

5. Corrosion properties

5.1 Stress corrosion

Fatigue pre-cracked DCB type specimens were loaded by a bolt up to an initial stress intensity of K_i = 9 MPa$\sqrt{m}$. Crack growth as a function of the exposure time was measured on both side surfaces of the specimen. Two specimens of each plate alloy for each condition were tested. Tuning fork type specimens were clamped on closely dimensioned plastic strips such that the maximum strain on the specimen apex was 0.3 %. During exposure the specimens were considered failed upon appearance of the first visible crack (inspection at 12.5 X magnification). Five specimens of each plate alloy for each condition were tested. The stress corrosion properties of the sheet materials were determined by exposing bent strips with maximum bending stresses of 300 MPa, 200 MPa and 100 MPa to the corrosive environment. A specimen was considered cracked when a crack could be identified at 12.5 X magnification. If crack growth occurred a specimen was considered failed when a clear kink in the curvature of the specimen was observed.

Stress corrosion crack initiation and crack growth in plate alloys was investigated for alternate immersion in synthetic seawater (ASTM G44-75) and outdoor exposure at the NLR. The test results in figure 11 show that for crack initiation alloy 8090-T651 was somewhat better than alloy 2024-T351 in both environments. Also, crack growth tests in synthetic seawater showed faster crack growth for alloy 2024-T351. However, outdoor exposure showed the opposite ranking. It appeared that in the accelerated corrosion test crack growth

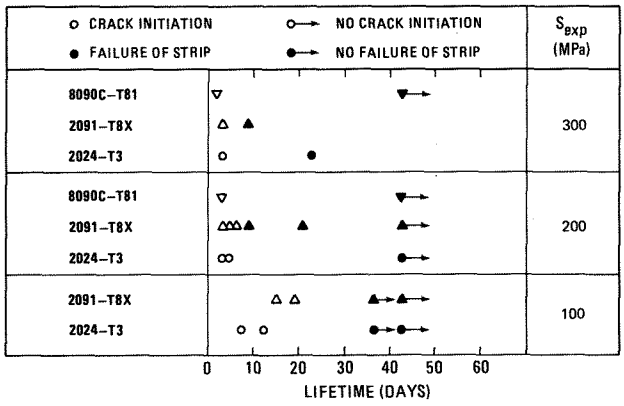

Fig. 12 Results of stress corrosion testing by alternate immersion in synthetic seawater

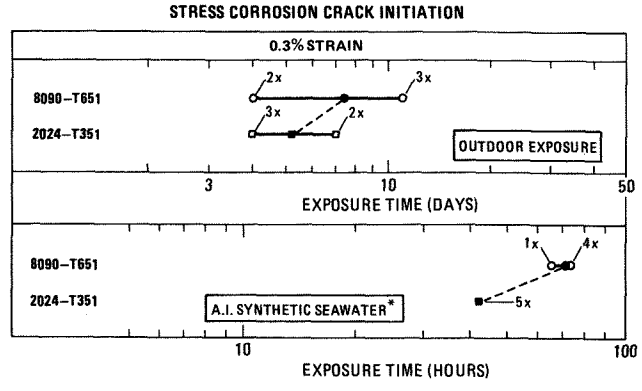

* 1 HOUR CYCLE: 10 MINUTES IMMERSED, 50 MINUTES DRY
RH = 45%, T = 27°C

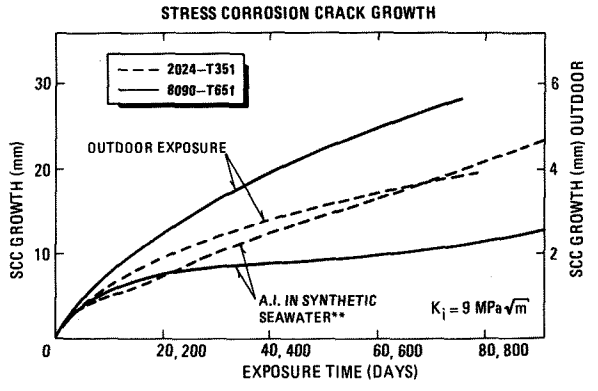

** 1 HOUR WET, 11 HOURS DRY
RH = 55%, T = 20°C

Fig. 11 Comparison of stress corrosion properties of 8090-T651 and 2024-T351 plate

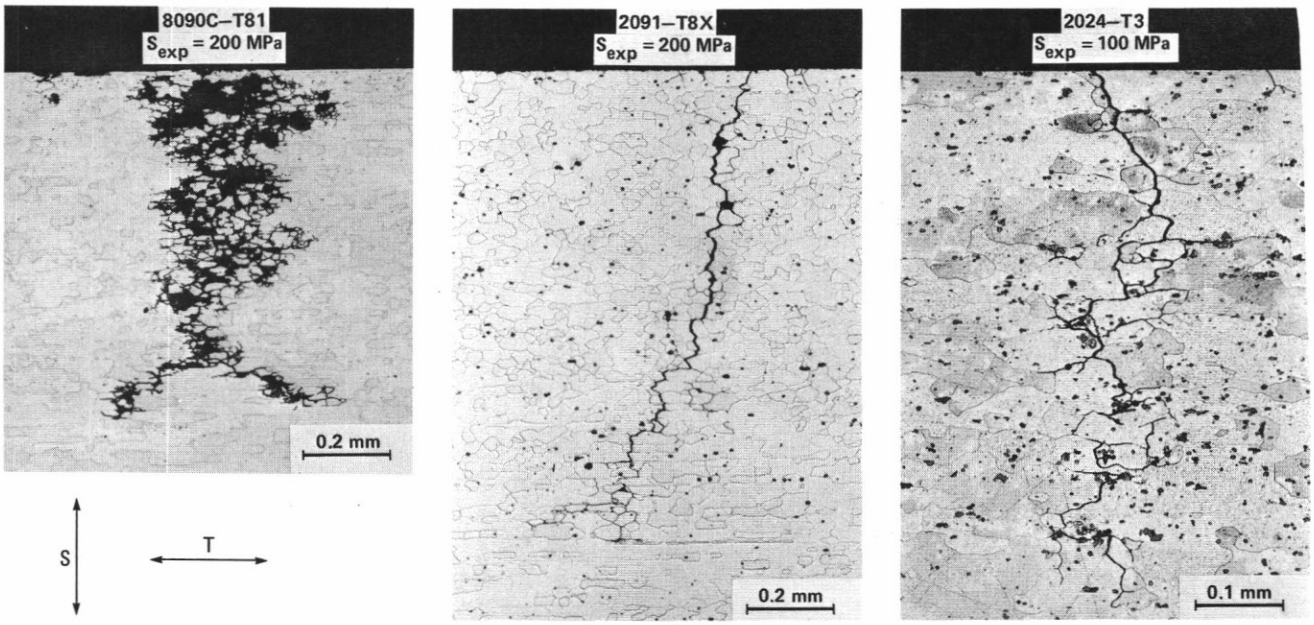

Fig. 13 Cross-sections showing the intergranular nature of the stress corrosion cracks in the different materials

was strongly influenced by corrosion product wedging (CPW) which was most pronounced for the alloy 2024 (4)(12). Voluminous corrosion products became the main crack driving force for stress corrosion crack growth in 2024-T351. In the natural environment the effect of CPW was less evident and the crack growth in 2024-T351 was less then that in 8090-T651.

Accelerated stress corrosion tests on the sheet materials, figure 12, showed that early crack initiation occurred in the Al-Li sheet alloys as well as in the reference alloy 2024-T3. But the initiated stress corrosion cracks grew much faster in 2091-T8X strips than in 2024-T3, while cracks in 8090C-T81 hardly grew at all. Cross-sections (Fig. 13) show the typical intergranular nature of stress corrosion cracks in 2091-T8X and 2024-T3. The finer grain structure of 2091-T8X provides an easier path for crack growth than that of 2024-T3, resulting in lower times to failure. In 8090C-T81 extensive crack branching resulted in a broad fissure with intergranular features rather than a stress corrosion crack. Note further the tendency for crack branching in 8090C-T81 and to some extent in 2091-T8X. The crack branching is related to incomplete recrystallization in the centre of the Al-Li alloy sheets.

5.2 General corrosion

Three types of corrosion tests were carried out:
- EXCO test according to ASTM-G-34-79
- MASTMAASIS test according to ASTM G85-85
- Outdoor exposure for one year.

The first two accelerated corrosion tests are frequently applied to determine the susceptibility to exfoliation corrosion. Details of the tests are given in references (5,12).

The results of the corrosion tests on plate and sheet materials are given in table 3. For plate materials EXCO testing resulted in more severe attack for 8090-T651 than for 2024-T351. However, the intermittent salt spray test (MASTMAASIS) showed a superior behaviour of 8090-T651 as compared to 2024-T351. Although the corrosion attack after 1 year of outdoor exposure was slight, the results so far indicate that 8090-T651 is less susceptible than 2024-T351. Thus the corrosion behaviour in a natural environment appears to be better represented by intermittent salt spray testing. For the sheet materials more or less the same results were obtained. Alloy 2091-T8X appeared to be slightly more susceptible to corrosion attack than 2024-T3.

	PLATE	SHEET*
EXCO, 48 hours	8090-T651 > 2024-T351	2091-T8X > 2024-T3
MASTMAASIS, 16 days	2024-T351 >> 8090-T651	2091-T8X $\hat{=}$ 2024-T3
OUTDOOR EXPOSURE, 1 year	2024-T351 > 8090-T651	2091-T8X > 2024-T3

* 8090C-T81 not tested

TABLE 3 SUSCEPTIBILITY TO CORROSION ATTACK UNDER DIFFERENT ENVIRONMENTAL CONDITIONS

6. Discussion

A number of damage tolerance and engineering properties were determined for the medium strength plate alloy 8090-T651, the damage tolerant sheet alloys 8090C-T81 and 2091-T8X, and the conventional sheet and plate alloys 2024-T3 and 2024-T351.

With respect to mechanical properties and fracture toughness the consistently lower fracture strains for the Al-Li alloys are a disadvantage. However, the plane strain and plane stress fracture toughnesses in the LT and TL orientations were good and comparable to those of 2024-T3 and T351. The poor short transverse fracture toughness of 8090-T651 is of concern, especially for multiaxially loaded components.

The Al-Li alloys were superior to 2024 in terms of notched fatigue strength and constant amplitude fatigue crack growth for a stress ratio R = 0.1. The latter superiority was explainable in terms of roughness-induced crack closure. This means that the superiority of Al-Li alloys is likely to decrease at higher R values. Clearly a more thorough evaluation of the fatigue crack growth properties is required before generalizing the results presented here. In this respect the flight simulation fatigue tests were most illustrative:

(1) 2024-T3 sheet was superior in flight simulation fatigue crack growth resistance as compared to damage tolerant Al-Li sheet materials.
(2) 8090-T651 plate was superior to 2024-T351 owing to the formation of separate crack fronts (transverse delamination). In turn, this delamination resulted from the poor short transverse properties. Improvement of the short transverse fracture toughness would therefore most likely decrease the fatigue crack growth resistance of 8090-T651 in the LT (and TL) orientation!

The stress corrosion and general corrosion properties of the Al-Li alloys were roughly equivalent to those of 2024-T3 and T351. In the case of stress corrosion this means that the overall resistance was low. It is desirable to improve the stress corrosion crack growth resistance of 2091-T8X sheet in order to make it an acceptable replacement for 2024-T3 in terms of stress corrosion behaviour.

Taking a total view of the results of the present investigation, it is evident that there is no simple answer to the question whether Al-Li alloys can replace conventional aluminium alloys in damage tolerant aircraft structures. An acceptable balance of properties in Al-Li alloys has not truly been achieved yet. In view of the complex inter-relationship of different properties, to some extent exemplified by the present results, this will be a formidable task.

7. Conclusions

An acceptable balance of properties in Al-Li alloys for use in damage tolerance aircraft structures has not yet been achieved. This will be a formidable task, as may be seen from the present results.

In more detail:

(1) Except for low fracture strains the mechanical properties and fracture toughnesses of the Al-Li alloy were generally comparable to those of 2024-T3 and T351. However, the low short transverse fracture toughness of 8090-T651 plate is of concern.
(2) The Al-Li alloys were superior to 2024 in terms of notched fatigue strength and constant amplitude fatigue crack growth for R = 0.1 (low positive stress ratio).
(3) The Al-Li alloys were generally inferior to 2024 in terms of flight simulation fatigue crack growth. 8090-T651 plate was, however, superior to 2024-T351 owing to the formation of separate, delaminated crack fronts. Improvement of the short transverse fracture toughness of 8090-T651 would probably prevent delamination and worsen the flight simulation fatigue crack growth resistance.
(4) The stress corrosion and general corrosion properties of the Al-Li alloys were roughly comparable to those of 2024-T3 and T351. However, the stress corrosion crack growth resistance of 2091-T8X should be improved.

8. Acknowledgement

This investigation has been sponsored by the Netherlands Agency for Aerospace Programs NIVR.

9. References

1. Sawtell, R.R., Bretz, P.E., Petit, J.I. and Vasudevan, A.K.,
Low density aluminium alloy development, Advanced Aerospace Materials Technology, SAE-SP-597, pp. 11-25, October, 1984.

2. Grimes, R., Cornish, A.J., Miller, W.S., and Reynolds, M.A.,
Aluminium-lithium based alloys for aerospace applications, Metals and Materials, pp. 357-363, June 1985.

3. Le Roy, G. and Meyer, Ph.,
Status of Al-Li development at Pechiney, Al-Li Symposium, Los Angeles, 25 - 26 March, 1987.

4. 't Hart, W.G.J. and Schra, L.,
Properties of the Al-Li plate alloy DTD XXXA-T651 (AA 8090-T651) in comparison with two damage tolerant 2000 series plate alloys, NLR TR 86115 L, November 1986.

5. Schra, L. and Boogers, J.A.M.,
Corrosion properties of Al-Li-Cu-Mg-Zr sheet materials, NLR 88047 L, March 1988.

6. Hyatt, M.V. and Speidel, M.O.,
Stress-corrosion cracking of high strength aluminium alloys, Advances in Corrosion Science and Technology, PLENUM Press, New York and London, Vol. 2, pp. 115-335, 1972.

7. -
Damage Tolerant Design Handbook,
A compilation of fracture and crack growth data for high-strength alloys, Metals and Ceramics Information Centre, Battelle Columbus Laboratories.

8. Broek, D. and Vlieger, H.,
The thickness effect in plane stress fracture toughness, NLR TR 74032 U, October 1973.

9. De Jonge, J.B., Schütz, D., Lowak, H. and Schijve, J.,
A standardized load sequence for flight simulation tests on transport aircraft wing structures, LBF Bericht FB-106, NLR TR 73029 U, March 1973.

10. Lowak, H., De Jonge, J.B., Franz, J. and Schütz, D.,
MINI-TWIST, a shortened version of TWIST, LBF-Report No. TB-146, NLR MP 79018 U, May 1979.

11. Wanhill, R.J.H.,
Gust spectrum fatigue crack propagation in candidate skin materials, Fatigue of Engineering Materials and Structures, Vol. 1, pp. 5-19, 1979.

12. Kolkman, H.J., 't Hart, W.G.J. and Schra, L.,
Additional investigation on the Al-Li plate alloy DTD XXXA-T651 (AA 8090-T651), NLR TR 87149 L, November 1987.